Current-Density Fluctuations and Ambipolarity of Transport

W. Shen, R. N. Dexter, and S. C. Prager
University of Wisconsin, Madison, Wisconsin 53706
(Received 7 October 1991)

The fluctuation in the plasma current density is measured in the MST reversed-field-pinch experiment. Such fluctuations, and the measured radial profile of the k spectrum of magnetic fluctuations, support the view that low-frequency fluctuations ($f < 30$ kHz) are tearing modes and high-frequency fluctuations (30 kHz $< f <$ 250 kHz) are localized turbulence in resonance with the local equilibrium magnetic field (i.e., $\mathbf{k}\cdot\mathbf{B}=0$). Correlation of current-density and magnetic fluctuations ($\langle\tilde{j}_\parallel\tilde{B}_r\rangle$) demonstrates that radial particle transport from particle motion parallel to a fluctuating magnetic field is ambipolar over the full frequency range.

PACS numbers: 52.55.Hc, 52.25.Fi, 52.35.Ra

The influence of magnetic fluctuations on plasma transport in magnetically confined plasmas is an unresolved problem of long-standing interest. The streaming of charged particles parallel to a fluctuating magnetic field is a powerful transport mechanism, particularly if the field lines wander stochastically in space [1,2]. Measurement of magnetic fluctuations in the edge of various toroidal plasmas suggests that they are important to transport in various settings, including reversed-field pinches [3], high-beta tokamaks [4], and tokamaks at the L-H transition [5]. However, experimental demonstration of the relation of these fluctuations to transport, as well as their identification, has been hampered by the scarcity of measurements of other fluctuating quantities, such as current density. Generally, the flux of a transport quantity is determined by the correlated product of two fluctuating quantities.

In this Letter we present two results on fluctuations and their relation to transport, through experiments in the MST reversed-field pinch. First, measurements of fluctuations in the current density have been obtained (using multicoil magnetic probes) over the outer 20% of the plasma radius. The diagnostic also yields the radial profile of the wave-number spectrum of magnetic-field fluctuations. These measurements are consistent with the view that low-frequency fluctuations ($f < 30$ kHz) are global tearing fluctuations and indicate that high-frequency fluctuations ($f > 30$ kHz) are localized modes resonant with the pitch of the highly sheared magnetic field (i.e., the resonance relation $m/n=q$ is locally upheld). Second, we have demonstrated that particle flux driven by magnetic fluctuations is ambipolar over the frequency range 5 kHz $< f <$ 250 kHz. It is obvious that flux driven by electrostatic turbulence is ambipolar since electrons and ions have identical $\mathbf{E}\times\mathbf{B}$ drifts in a fluctuating electric field. These fluxes have been measured in the edge of many toroidal devices. However, the response of particles to magnetic fluctuations is mass dependent since it depends upon the parallel particle speed; hence, the differential loss rate of electrons and ions is determined by properties of the turbulence. Theoretical works have discussed the issue [1,6–8] and predict ambipolarity in the presence of microturbulence [8]. We affirm this experimentally, and also measure ambipolarity in the presence of global tearing modes. The difference between the ion and electron particle radial fluxes (Γ_i and Γ_e) driven by particle motion parallel to a fluctuating magnetic field is proportional to the correlated product of the parallel current-density fluctuations $\tilde{j}_\parallel$ and the radial magnetic-field fluctuations $\tilde{B}_r$; i.e., $\Gamma_i-\Gamma_e \propto \langle\tilde{j}_\parallel\tilde{B}_r\rangle$. We measure this correlated term to be zero, to within the experimental uncertainty. The upper bound on the nonambipolar flux is about 5% of the total flux.

The MST reversed-field-pinch plasma [9,10] has a plasma minor radius of 0.51 m, a major radius of 1.5 m, and is separated from a conducting wall (5-cm-thick aluminum) by graphite limiters which extend 1 cm from the wall. The data presented here were obtained at low plasma current (≈ 220 kA) with plasma duration ≈ 60 ms, field-reversal parameter ≈ -0.15, pinch parameter ≈ 1.7, line-averaged-electron density $\approx 0.8\times10^{13}$ cm^{-3}, central electron temperature ≈ 150 eV, and global energy and particle confinement times of roughly 1 ms.

The current density is obtained by measuring the magnetic field with an array of pickup coils, and taking appropriate differences to approximate curl $\mathbf{B}$. For example, the poloidal current density is obtained from two radially separated, toroidally oriented coils and two toroidally separated, radial coils. The diagnostic consists of two poloidal, four toroidal, and two radial magnetic coils distributed within two parallel tubes to minimize probe perturbation to the plasma current. The tubes are 0.9 cm in diameter, are separated by 1.7 cm, and are mounted on a common movable stalk for insertion within the plasma. The coils, with 0.2-cm radii, have separations between 0.5 and 1.7 cm. Signals are digitized at a 500-kHz sampling rate, and integrated using fast Fourier transforms. Ensemble averages are formed with about 250 time records, each of 500-μsec duration, accumulated from about 50 reproducible discharges. The wavelength resolution, limited by the coil spacing, is sufficient to cover wavelengths corresponding to the full available frequency range. The magnetic fluctuations are measured to 1% accuracy, limited by accuracy in the coil alignment and calibration of the effective area. The current-density fluctuations are obtained from magnetic-

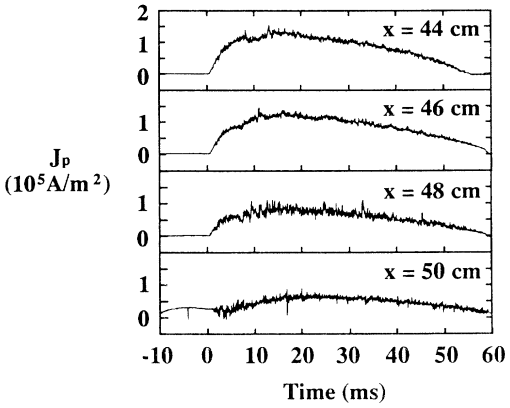

FIG. 1. Time dependence of poloidal current density at four radial locations. The equilibrium component of the current density is accurate to 2%.

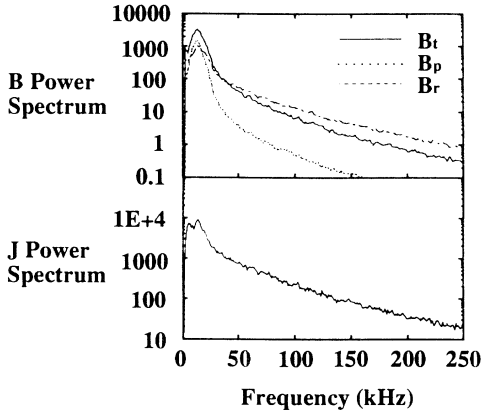

FIG. 2. Frequency dependence of fluctuations in magnetic field and poloidal current density. The magnetic-field and current-density fluctuations are measured to an accuracy of 1% and 15%, respectively.

field differences of typically 7% to 10%. Hence, the alignment inaccuracy yields roughly a 15% inaccuracy in $\tilde{j}$. Equilibrium current density is measured to an accuracy of 2%. Errors in electronic amplification and digital differencing are small ($<1\%$). The errors in the magnitude and phase of the coherence between two signals are both 5%, arising from the finite ensemble size. The probe is inserted from the wall to a minor radius of 42 cm ($r/a=0.82$) without adversely affecting plasma parameters. The time dependence of the poloidal current density (which is nearly parallel to B in the outer region) is shown in Fig. 1. The magnitude and radial dependence of the equilibrium current density agrees with expectation from MHD equilibrium modeling.

The frequency spectra of current-density and magnetic fluctuations are displayed in Fig. 2. The current-density spectrum is broader than the magnetic fluctuations, as expected since $\tilde{j}$ and $\tilde{B}$ are related through wave number k, which is observed (as described below) to increase with frequency. For ease of categorization we separate the spectrum into a low-frequency range ($f<30$ kHz), which contains the dominant peak, and a high-frequency range (30 kHz $<f<250$ kHz). From edge magnetic fluctuation measurements in past devices, as well as MST, the low-frequency range has long been identified as tearing fluctuations, since the dominating spatial modes are as predicted by nonlinear MHD computation [11]. The current-density measurements are consistent with this view. The relative phase angles between j and B (zero radians between j_p and B_p, $-\pi/2$ between B_p and B_r, and π between B_p and B_t) agree with the prediction for tearing modes. In addition, the ratio of $\tilde{j}/j$ to $\tilde{B}/B$ is about 4 in both experiment and computation. However, the magnitudes of the fluctuations in the experiment ($\tilde{j}/j\approx 0.1$ and $\tilde{B}/B\approx 0.02$) are about half that predicted in computation (which operates with a Lundquist number about 100 times smaller than the experimental value). The dominant low-frequency fluctuations are relatively coherent in time as indicated in Fig. 3.

An indication of the global nature of the low-frequency fluctuations is indicated in Fig. 4(a) which displays the poloidal and toroidal mode number (m and n) spectra at two different radii, $r=42$ cm and $r=46$ cm. The spectra are approximated from a two-point phase shift measurement [12]. At low frequency the two-point results agree with more accurate spectra which were obtained with the fields measured at 64 toroidal locations and 16 poloidal locations. The central safety factor is roughly 0.23 (from equilibrium modeling) and the edge safety factor is about -0.03. The reversal surface where the safety factor q changes sign is located at $r\approx 44$ cm. The low-frequency spectra are relatively unchanging with radius from $r=42$ cm to the wall. Since $m/n>0$, the modes are resonant in the plasma core and global.

In contrast, the high-frequency fluctuations vary substantially with radius, as shown in Fig. 4(b). The n spectrum is broad and at $r=46$ cm, $m/n<0$, indicating that the modes are locally resonant at the edge. The n values

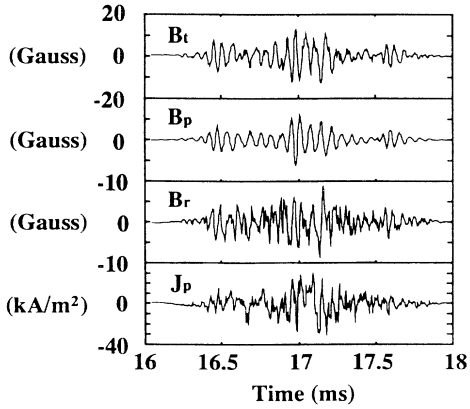

FIG. 3. Time dependence of fluctuations in magnetic field and current density, illustrating relatively coherent oscillations at low frequency. Magnetic and current-density fluctuations are accurate to 1% and 15%, respectively.

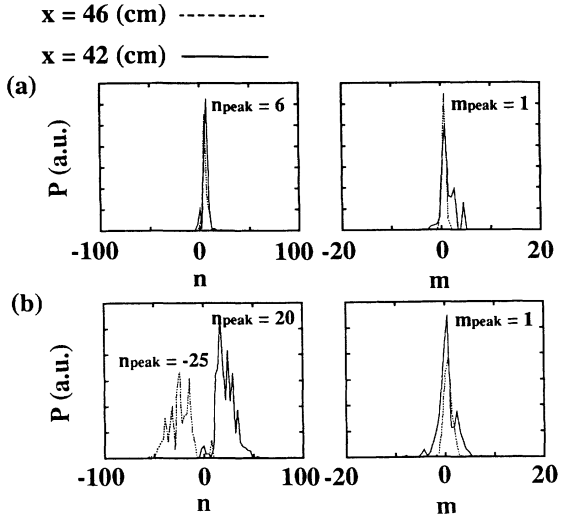

FIG. 4. Mode number spectra of magnetic fluctuations. (a) Spectra at low frequency (5 kHz to 50 kHz) and (b) spectra at high frequency (50 kHz to 250 kHz). The dashed lines correspond to minor radius $r=46$ cm, and the solid lines to $r=42$ cm. The poloidal and toroidal mode numbers are denoted by m and n, respectively. The values of m and n at the peaks are indicated in the figures.

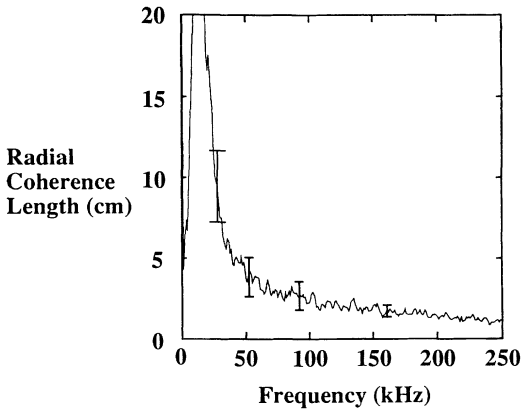

FIG. 5. Radial coherence length of toroidal magnetic fluctuations at $r=46$ cm. The coherence length is the e-folding length of the ensemble-averaged coherence measured between two radial locations. Similar results are obtained for the poloidal magnetic field.

(and m/n) reverse sign from $r=46$ cm to $r=42$ cm, thereby maintaining local resonance with the field line pitch which also changes sign at $r\approx 44$ cm. The radial coherence length, obtained from the ensemble-averaged coherence between the field at two radial locations, decreases with frequency (Fig. 5), to the cm scale at high frequency. Hence, we characterize the high-frequency range as localized, resonant turbulence.

The ion and electron particle fluxes in the radial direction arising from magnetic fluctuations are commonly expressed (for $\omega \ll \omega_c$, the cyclotron frequency) as

$$\Gamma_i = \langle \tilde{j}_{i\parallel} \tilde{B}_r \rangle / eB, \quad \Gamma_e = -\langle \tilde{j}_{e\parallel} \tilde{B}_r \rangle / eB , \tag{1}$$

where $\tilde{j}_{i\parallel}$ and $\tilde{j}_{e\parallel}$ are the ion and electron current-density fluctuations parallel to the magnetic field, and $\langle\,\rangle$ denotes an ensemble average over fluctuating quantities, which are superscripted by a tilde. Other transport mechanisms, such as $\mathbf{E}\times\mathbf{B}$ transport, are not displayed and would enter into Eq. (1) additively. From a kinetic viewpoint [13], these fluxes arise from particles streaming parallel to a fluctuating magnetic field. The parallel flux of guiding centers, given by the drift kinetic equation, is $\Gamma_\parallel = \int v_\parallel (\mathbf{B}/B) f(v_\parallel) dv_\parallel = j_\parallel (\mathbf{B}/B)/e$. The radial component of the parallel flux is $\Gamma_r = \boldsymbol{\Gamma}_\parallel \cdot \hat{\mathbf{r}}$, which yields Eq. (1) after perturbing and averaging. This expression describes particle transport from parallel motion no matter what the underlying structure of the magnetic field. It includes, but is not limited to, particle transport arising from a stochastic magnetic field [1,2]. From a two-fluid viewpoint [8], the radial flux is obtained from the ensemble-averaged momentum equation for each species if we ignore the inertial term and include only the Lorentz force (the inertial term can contribute an additional flux, but is not the subject of the present work). Taking the component in the direction mutually perpendicular to the equilibrium field and the radial direction we obtain $\langle \mathbf{j}\times\mathbf{B}\rangle \cdot (\hat{\mathbf{b}}\times\hat{\mathbf{r}}) = 0$. Decomposing the averaged quantity into its mean and fluctuating parts yields $\langle j_r\rangle\langle B\rangle - \langle \tilde{j}_\parallel \tilde{B}_r\rangle = 0$. We have ignored the term $\langle \tilde{j}_r \tilde{B}_\parallel \rangle$ since this is a mechanism separate from the parallel streaming effect considered in this paper. Furthermore, this term is usually considered to be small, which we anticipate is the case in MST. Solution for $\Gamma_r = j_r/e$ yields Eq. (1). The radial fluid flow can be considered to be driven by an $\mathbf{F}\times\mathbf{B}$ drift in which the force $\mathbf{F}$ is the ensemble-averaged Lorentz force $\langle \tilde{\mathbf{j}}_\parallel \times \tilde{\mathbf{B}}_r \rangle$.

The nonambipolar component of the particle flux is

$$\Gamma_i - \Gamma_e = \langle \tilde{j}_\parallel \tilde{B}_r \rangle / eB , \tag{2}$$

where $\tilde{j}_\parallel = \tilde{j}_{i\parallel} + \tilde{j}_{e\parallel}$. We can decompose $\tilde{j}_\parallel$, the perturbation in $\mathbf{j}\cdot\mathbf{B}/B$, as $\tilde{j}_\parallel = (1/B)(\tilde{j}_p B_p + \tilde{j}_t B_t + j_p \tilde{B}_p + j_t \tilde{B}_t - \mathbf{j}\cdot\hat{\mathbf{b}}\tilde{B})$. We measure each of the five terms. The first term dominates. The last three terms are small since $\tilde{B}/B \ll \tilde{j}/j$, and the second term is small in the edge region where B_t is small. The frequency spectrum of the magnitude and phase of the nonambipolar component of the flux [Eq. (2)] is shown in Fig. 6. We see that $\tilde{j}_\parallel$ and $\tilde{B}_r$ have a phase difference of $\pi/2$ at all frequencies, indicating that $\Gamma_i \approx \Gamma_e$ and the flux is ambipolar. The individual magnitudes of $\tilde{j}_\parallel$ and $\tilde{B}_r$ are sufficiently large that the nonambipolar flux would be substantial if the phase difference were zero. Considering the 5% inaccuracy in the phase measurements we put an upper bound on the nonambipolar flux of 5×10^{19} m^{-2}sec^{-1}, which is about a factor of 20 smaller than the actual particle flux. Hence, the flux is ambipolar to good accuracy.

In the low-frequency range we interpret the ambipolarity as being necessitated by the phase relations of the

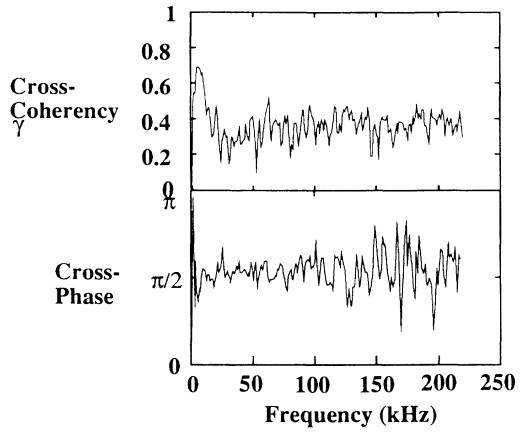

FIG. 6. Magnitude and phase of the ensemble-averaged coherence, $\langle \tilde{j}_\parallel \tilde{B}_r \rangle / (|\tilde{j}_\parallel|^2 |\tilde{B}_r|^2)^{1/2}$. The magnitude and phase are both accurate to 5%.

tearing mode discussed earlier. The key phase relation is seen from Ampere's law, $\mu_0 \tilde{j}_p = \partial \tilde{B}_t / \partial r - (1/R) \partial \tilde{B}_r / \partial \varphi$. For a global tearing mode, the wave is radially standing and toroidally propagating. Hence, the second term on the right-hand side is out of phase with $\tilde{B}_r$. The first term is in phase with $\tilde{B}_t$, which by the solenoidality of B (and invoking the known π phasing between $\tilde{B}_t$ and $\tilde{B}_p$) is out of phase with $\tilde{B}_r$. Thus, the left-hand side, $\tilde{j}_p$, is out of phase with $\tilde{B}_r$.

The ambipolarity at high frequency can be somewhat explained using the simple argument of Waltz [8]. He considers localized modes for which the fluctuating magnetic field is transverse to the equilibrium magnetic field ($\tilde{B}_\parallel = 0$). This condition is well satisfied for the measured fluctuations for which $\tilde{B}_\parallel / \tilde{B}_\perp \approx \tilde{B}_p / \tilde{B}_r \approx 0.02$. For this case, a consequence of Ampere's law is that $\langle \tilde{j}_\parallel \tilde{B}_r \rangle$ vanishes upon integration over the narrow radial width of a mode [8]. This result is consistent with, but is less stringent than, the experimental result. In experiment $\langle \tilde{j}_\parallel \tilde{B}_r \rangle$ is pointwise zero, subject to the radial averaging effect of the finite radial extent of the diagnostic, which is about 1 cm, less than the radial correlation length of the turbulence. The pointwise ambipolarity is not a consequence of Ampere's law alone, but results from magnetic phase relations which depend on the nature of the turbulence. If the fluctuations were propagating toroidally and nonpropagating radially, and if $\tilde{B}_p \approx \tilde{B}_\parallel$ were negligible in the div**B** equation, then the required phase relation follows from Ampere's law as described above for tearing modes. A full explanation of the ambipolarity might require a more complete treatment of the turbulence. For example, an equilibrium radial electric field can alter the fluctuations and the differential loss of electrons and ions [1].

In summary, we have obtained measurements of current-density fluctuations which provide new identifying features of magnetic fluctuations and allow determination of the ambipolarity of particle transport. At low frequency, the current-density fluctuations are large ($\tilde{j}/j \approx 0.1$) and identifiable as tearing modes. At high frequency, the current fluctuations are modest ($\tilde{j}/j < 2 \times 10^{-3}$ for $f > 50$ kHz) and are localized, resonant turbulence. The k spectrum of the high-frequency turbulence changes dramatically with radius, maintaining local resonance with the equilibrium field. The differential loss rate of ions and electrons is measured by correlating $\tilde{j}_\parallel$ with $\tilde{B}_r$. It is shown that the particle loss from magnetic fluctuations is ambipolar. This is expected at low frequency from the phase relation between $\tilde{j}$ and $\tilde{B}$ of tearing modes. It had been predicted that particle flux from localized turbulence is ambipolar upon radial average over a mode width. This provides partial explanation of the experimental result at high frequency. In the experiment a more stringent ambipolarity holds since the only radial averaging is from the radial resolution of the diagnostic, which is less than the radial correlation length of the turbulence. If we assume that the ion current-density fluctuation is small [$\tilde{j}_i \approx \tilde{j}(m_e/m_i)^{1/2}$], then ambipolarity leads to the conclusion that magnetic-fluctuation-induced particle transport is small compared to the actual particle flux. Confirmation of this expectation awaits measurement of the fluctuations in current density of the individual species.

The authors are grateful to James Callen, Paul Terry, and Nathan Mattor for useful discussions, to Elizabeth Zita for provision of MHD computational results, and to Saeed Assadi and Trudy Rempel for important advice on data analysis. The work is supported by the U.S. Department of Energy.

[1] J. D. Callen, Phys. Rev. Lett. **39**, 1540 (1977).
[2] A. B. Rechester and M. N. Rosenbluth, Phys. Rev. Lett. **40**, 38 (1978).
[3] See, for example, I. H. Hutchinson *et al.*, Nucl. Fusion **24**, 59 (1984).
[4] B. A. Carreras *et al.*, Phys. Rev. Lett. **50**, 503 (1983).
[5] N. Ohyabu *et al.*, Phys. Rev. Lett. **58**, 120 (1987).
[6] W. M. Mannheimer and I. Cook, Comments Plasma Phys. **5**, 5 (1979).
[7] S. Inoue *et al.*, Nucl. Fusion **19**, 1252 (1979).
[8] R. E. Waltz, Phys. Fluids **25**, 1269 (1982).
[9] R. N. Dexter *et al.*, Fusion Technology **19**, 131 (1991).
[10] S. C. Prager *et al.*, Phys. Fluids B **2**, 1367 (1990).
[11] See, for example, D. D. Schnack *et al.*, Phys. Fluids **28**, 321 (1985); also, E. J. Zita (private communication).
[12] J. M. Beall *et al.*, J. Appl. Phys. **53**, 3933 (1982).
[13] See, for example, P. C. Liewer, Nucl. Fusion **25**, 543 (1985).